Proc. Natl. Acad. Sci. USA
Vol. 93, pp. 10632–10637, October 1996
Biochemistry

Mutations in the C-terminal fragment of DnaK affecting peptide binding

WILLIAM F. BURKHOLDER*†, XUN ZHAO†, XIAOTIAN ZHU†‡, WAYNE A. HENDRICKSON†‡, ALEXANDER GRAGEROV*†§, AND MAX E. GOTTESMAN*†¶

†Department of Biochemistry and Molecular Biophysics and *Institute of Cancer Research, 701 West 168th Street, Room 914, and ‡Howard Hughes Medical Institute, 650 West 168th Street, Room 203, Columbia University, New York, NY 10032

Contributed by Wayne A. Hendrickson, July 5, 1996

ABSTRACT ***Escherichia coli*** **DnaK acts as a molecular chaperone through its ATP-regulated binding and release of polypeptide substrates. Overexpressing a C-terminal fragment (CTF) of DnaK (Gly-384 to Lys-638) containing the polypeptide substrate binding domain is lethal in wild-type *E. coli*. This dominant-negative phenotype may result from the nonproductive binding of CTF to cellular polypeptide targets of DnaK. Mutations affecting DnaK substrate binding were identified by selecting noncytotoxic CTF mutants followed by *in vitro* screening. The clustering of such mutations in the three-dimensional structure of CTF suggests the model that loops $\mathcal{L}_{1,2}$ and $\mathcal{L}_{4,5}$ form a rigid core structure critical for interactions with substrate.**

Hsp70s, including *Escherichia coli* DnaK, bind nascent and unfolded polypeptides to prevent premature folding or aggregation during translation, to promote translocation into organelles, or to target polypeptides for proteolysis (1–4). In addition, DnaK and other hsp70s recognize certain native protein substrates, maintaining them in active or inactive conformations or disassembling them from oligomeric complexes. Consistent with their role as molecular chaperones, hsp70s bind a wide variety of model peptide substrates, exhibiting a strong preference for sequences enriched in hydrophobic residues (5–8), which would normally be buried in folded polypeptides. The ADP-bound form of hsp70s has a high affinity for polypeptide substrates and forms stable complexes with slow dissociation rates (9–14). Exchange of ADP for ATP induces substrate dissociation and shifts hsp70s to a low affinity form in parallel with conformational changes in the ATPase and core substrate binding domains (9–20). Hydrolysis of ATP to ADP, stimulated by substrate binding, results in a new round of stable complex formation

Hsp70s consist of three domains: (*i*) an N-terminal ATPase domain (DnaK residues 1 to ≈385), (*ii*) a proximal C-terminal domain (≈386 to ≈538) containing the core substrate binding site, and (*iii*) a distal C-terminal domain (≈539 to 638) that may include the binding site for the cofactor DnaJ and its homologues (7, 21–26). We have recently reported the crystal structure of a C-terminal fragment of *E. coli* DnaK (CTF; residues 389–607) bound to a peptide substrate (27). The CTF consists of a β-sandwich, containing the substrate binding channel, followed by five α-helices. The substrate peptide is encapsulated in an extended conformation between two loops, $\mathcal{L}_{1,2}$ and $\mathcal{L}_{3,4}$, which are in turn buttressed by two other loops, $\mathcal{L}_{4,5}$ and $\mathcal{L}_{5,6}$. All four loops are formed by distortion of the four strands of one of the β-sheets. The first, short α-helix (helix αA), packs against loop $\mathcal{L}_{4,5}$, which stabilizes loop $\mathcal{L}_{1,2}$, and the second, long α helix (helix αB), passes over all four loops, latching closed the substrate binding channel formed by the loops. The remaining three α-helices pack against the distal end of helix αB, forming a second discrete domain. The structure of a second crystal form of the CTF shows that helix αB can kink, eliminating its contacts with the outer loops, $\mathcal{L}_{3,4}$ and $\mathcal{L}_{5,6}$, which in turn exhibit greater mobility in the second crystal structure. This suggests a mechanism by which the peptide binding channel can be opened and closed.

We have shown previously that a histidine-tagged fragment of DnaK (Gly-384 to Lys-638, referred to as CTF), containing both the proximal and distal C-terminal domains, binds a variety of model peptide substrates with the same affinities as ADP-bound full-length DnaK, and with equally slow substrate dissociation rates (7). Similar results have been obtained with related CTFs of DnaK and other hsp70s (19, 22, 25). We have used a genetic approach to identify sites in CTF required for peptide binding. Many of the mutations isolated cluster in the region of the inner loops, $\mathcal{L}_{1,2}$ and $\mathcal{L}_{4,5}$, which we interpret as strong independent evidence for the model that the inner loops form a rigid core domain in contrast to the greater flexibility of the outer loops.

MATERIALS AND METHODS

Bacterial Strains, Media, and Plasmids. CTF mutants were selected and studied *in vivo* using strain GA45 [LE392 Δ*lac*, expressing *lac* repressor from the compatible kan^R plasmid pREP4 (Qiagen)]. The ability of mutant alleles of full-length *dnaK* to complement the growth and λ phage plating defects of a Δ*dnaK* strain were screened using strains BB205 [a derivative of strain BB1553, MC4100 Δ*dnaK52*::cam^R *sidB1* expressing *lac* repressor from the compatible tet^R plasmid, pBB42 (28)], and BB209 (an isogenic $dnaK^+$ derivative of strain BB205 lysogenized with a λimm^{434} prophage expressing $dnaK^+$ from the *dnaK* promoter). GA45, BB205, and BB209 carry deletions of the *lac* operon that eliminate *lacY*, encoding lactose permease. IPTG thus enters these cells only by diffusion, allowing titratable control of *lac* promoter activity. Strains were grown in LB medium (29) supplemented with antibiotics as required, at the following concentrations: 50 μg/ml ampicillin, 25 μg/ml chloramphenicol, 25 μg/ml kanamycin, and 15 μg/ml tetracycline.

The CTF expression plasmid, pDKCT, was derived from a previously described plasmid (7) by replacing its amp^R marker with the tet^R marker from pACYC184, to eliminate background satellite colonies in the selection for CTF mutants. A tet^R control plasmid that does not express CTF, pBB43, was derived from the parent vector.

The *dnaK* expression plasmid, pBB46, was constructed from a 5′ fragment of the *dnaK* gene (nucleotides 1–1155) amplified

The publication costs of this article were defrayed in part by page charge payment. This article must therefore be hereby marked "*advertisement*" in accordance with 18 U.S.C. §1734 solely to indicate this fact.

Abbreviations: CTF, C-terminal fragment of DnaK; IPTG, isopropyl-β-D-thiogalactopyranoside.

§Present address: Advanced BioScience Laboratories Basic Research Program, National Cancer Institute–Frederick Cancer Research and Development Center, P.O. Box B, Building 539, Frederick, MD 21702-1201.

¶To whom reprint requests should be addressed. e-mail: gottesman@cuccfa.ccc.columbia.edu.

by the polymerase chain reaction and cloned into the expression plasmid pQE60 (Qiagen). The 3′ end of the *dnaK* insert in pQE60 was removed distal to the *Rsr*II site of *dnaK* and replaced with the *Rsr*II–*Dra*I fragment of the *dnaKJ* operon, subcloned from plasmid pJM2 (30), thus reconstituting the full-length *dnaK* gene. The *Rsr*II–*Dra*I fragment contains the 3′ end of *dnaK* and most of the intergenic region between *dnaK* and *dnaJ*. The his_6 tag present in pQE60 was not fused to full-length DnaK and lies downstream of the *dnaK* stop codon. Mutations were introduced by oligonucleotide-directed mutagenesis, and *Rsr*II–*Sal*I fragments of *dnaK* containing the mutations were recloned into the *dnaK* expression plasmid, pBB46. Mutations and ligation joints were verified by sequencing.

Selection of CTF Mutants. pDKCT DNA (10–20 μg) was incubated in 0.5 M sodium phosphate, 0.4 M hydroxylamine·HCl (HA), and 1 mM EDTA (adjusted to pH 6.0 with NaOH) at 56°C (31). Samples were taken after 4 h of incubation, applied to Quick Spin Sephadex G-25 spun-chromatography columns (Boehringer Mannheim), equilibrated in 10 mM Tris·HCl (pH 8.0) and 1 mM EDTA to remove HA, and transformed into strain GA45. Transformants were selected on LB plates supplemented with antibiotics and 5 μM isopropyl-β-D-thiogalactopyranoside (IPTG) at 42°C. DNA untreated with HA yielded no transformants under these selection conditions, while yielding fivefold more transformants than the HA-treated DNA in control platings at 30°C. Mutants selected for further study following *in vitro* screening were retransformed into strain GA45 to verify that the mutations were plasmid-linked. Mutations were then identified by sequencing the entire coding region of each plasmid on one strand and differences from the wild-type sequence were confirmed by sequencing regions of the complementary strand.

Purification of Wild-Type and Mutant CTF Proteins. Overnight cultures grown at 30°C in the presence of 0.2% glucose were diluted 100-fold into fresh media without glucose, grown to OD_{600} 0.2–0.3, and induced for 2 h with 1 mM IPTG before harvesting. Cell pellets were resuspended in 50 mM sodium phosphate (pH 8), 300 mM NaCl, 0.1% Tween 20, and 30 mM imidazole, and sonicated. The cleared lysates were incubated with Ni^{2+}-NTA resin (Qiagen) for 1 h at 4°C with mixing. The resin was then washed repeatedly in batch with 50 mM sodium phosphate (pH 6.1), 300 mM NaCl, 0.1% Tween 20, 45 mM imidazole, and 5% glycerol. Finally, bound protein was eluted in a final concentration of 200–250 mM imidazole in the same buffer. Samples were usually exchanged into 20 mM Tris·HCl (pH 8.0), 100 mM KCl, 5 mM $MgCl_2$, 5 mM 2-mercaptoethanol, and 5% glycerol, by spun-column chromatography or in Centricon-10 microconcentrators.

Preparation of Soluble and Insoluble Fractions of Cell Lysates. Samples (10 ml) of each culture were centrifuged and cell pellets were resuspended in 400 μl 20 mM Tris·HCl (pH 8.0), 100 mM NaCl, 5 mM 2-mercaptoethanol, and 1 mM phenylmethylsulfonyl fluoride (PMSF). Cells were disrupted by sonication, and insoluble cell debris was pelleted by centrifugation at 15,000 × *g* for 10 min at 4°C. Supernatants were saved, and pellets were resuspended and sonicated again until a negligible fraction of protein was released into the supernatant. Pellets were then washed twice in lysis buffer before they were resuspended in 50 μl SDS loading buffer and boiled.

Measurement of Peptide Binding by Dialysis. Ni^{2+}-NTA purified CTFs (15 μM) of roughly equal purity (95% by densitometry of Coomassie blue-stained gels) were mixed with buffer (filter-sterilized 20 mM Tris·HCl, pH 8.0/100 mM KCl/5 mM $MgCl_2$/0.1% Tween 20/0.02% sodium azide) containing 1 μM ^{3}H-labeled peptide NR (NRLLLTG; ref. 7) (≈6000 cpm per 40 μl sample) and dialyzed against buffer containing 1 μM [^{3}H]NR using an Original Microdialysis System (Pierce) and Spectra/Por 7 dialysis membrane (Spectrum; 25 kDa molecular weight cutoff). Ten 70–80 μl samples were dialyzed at a time against *ca.* 30 ml buffer at room temperature with mixing of the chamber buffer. The distribution of labeled peptide between the sample wells and the chamber was then determined by liquid scintillation counting. Control experiments showed that equilibrium was reached within 20 h with no detectable degradation of proteins. Protein concentrations were determined by Bio-Rad Protein Assay and by densitometry of Coomassie blue-stained gels.

Complementation Screening. Strains BB205 (Δ*dnaK52*) and BB209 (an isogenic *dnaK*$^+$ derivative of strain BB205) were transformed with pQE60 (vector), pBB46 expressing *dnaK*$^+$ from a synthetic *lac* promoter (p*dnaK*$^+$), or derivatives of pBB46 carrying the indicated point mutations. Transformants were selected at 30°C and screened for growth at the indicated temperatures by restreaking single colonies of each strain on LB plates supplemented with antibiotics and IPTG. Plates were evaluated after a 1-day incubation at 30–42°C and after a 4-day incubation at 16°C.

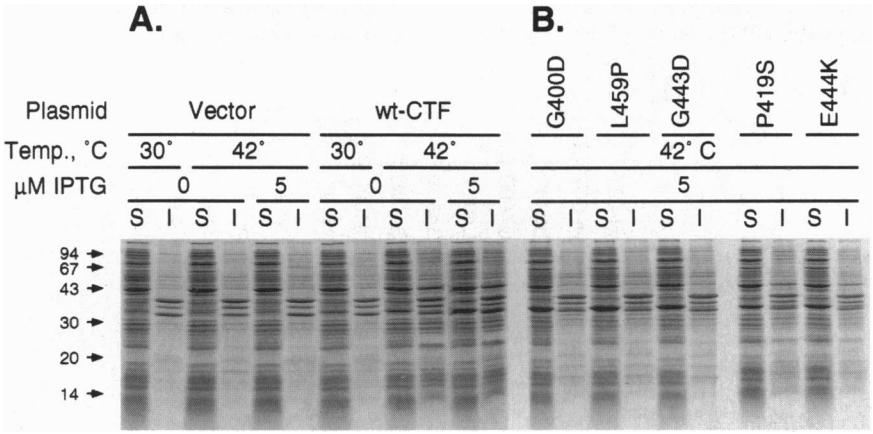

FIG. 1. (*A*) Aggregation of proteins in cells overexpressing wild-type CTF at 42°C. Overnight cultures of strain GA45 carrying the CTF expression plasmid, pDKCT, or a control plasmid that did not express CTF, pBB43, were grown at 30°C, diluted into fresh media to an OD_{600} of 0.03, and grown to an OD_{600} of 0.2 before removing samples, shifting to 42°C, and, where indicated, adding 5 μM IPTG. Cells were maintained in exponential phase growth between OD_{600} 0.02 and 0.5 by dilution and were harvested 1.5 h after the shift to 42°C. Soluble (S) and insoluble (I) fractions of sonicated cell lysates were prepared, separated on 15% SDS polyacrylamide gels, and stained with Coomassie blue. Soluble lysate (8 μg) was loaded in each lane, and an equal volume of the corresponding insoluble fraction (resuspended and boiled in SDS-loading buffer) was loaded in the adjacent lane. Note that insoluble fractions were eightfold more concentrated than soluble fractions. Molecular weight markers are indicated. Aggregation of low molecular weight proteins is particularly noticeable. (*B*) Aggregation of proteins in cells overexpressing selected mutant CTFs. Samples were prepared in parallel with the wild-type and control samples shown in *A*. Data for other mutant CTFs are not shown.

RESULTS

Selection of CTF Mutants. Overproduction of CTF was toxic to *E. coli* at 42°C. Even basal expression of CTF in the absence of inducer was sufficient to cause marked aggregation of soluble proteins when cells were shifted from 30°C to 42°C (Fig. 1*A*). Inducing CTF expression with 5 μM IPTG while shifting cells from 30°C to 42°C blocked growth after 1.5 h, and the induced cells filamented (data not shown). Control cells carrying vector alone displayed none of these phenotypes.

Since overexpressed CTF is fully functional for peptide binding *in vitro*, we believe that the *in vivo* phenotypes of CTF induction result from the formation of complexes between CTF and endogenous targets of DnaK. As with peptide substrates *in vitro,* CTF would dissociate slowly from these complexes, thus inhibiting the folding or activity of bound substrates and/or blocking their accessibility to functional endogenous DnaK. The phenotypes of CTF induction, filamentation, and protein aggregation are in fact reminiscent of *E. coli* strains defective in chaperone function (32–34). We therefore expected that a subset of CTF mutants selected as noncytotoxic should be defective in substrate binding.

CTF mutants were selected by treating the CTF expression plasmid with hydroxylamine and isolating transformants able to grow at 42°C in the presence of 5 μM IPTG. Of the 151 colonies isolated, 47 produced little or no CTF or amber fragments of the protein. CTFs were affinity-purified from the remaining transformants on Ni^{2+}-NTA agarose (Qiagen) for screening *in vitro*.

***In Vitro* Screening of CTF Mutants.** DnaK and CTF self-associate into oligomeric complexes (35–41) that dissociate upon addition of a substrate peptide (refs. 35–40; X. Zhao, unpublished work), and this can be monitored by native gel electrophoresis (Fig. 2). Self-binding may be mediated by the same site as substrate binding, in which case binding-defective mutants might display altered equilibria of self-association. We therefore screened the purified CTF mutants on native gels. Thirty-seven mutants exhibited mobilities distinct from wild type. The CTF coding regions of the plasmids expressing these mutant CTFs were sequenced, and all carried single missense mutations. Altogether, 15 mutations occurring at 13 residues were identified (Table 1; Fig. 2). Of these, 10 mutations reduced the affinity of purified CTF for peptide NR from twofold to greater than sevenfold (Table 1). Except for mutant G406D, the levels of CTF expression from the mutant plasmids were equivalent to the levels of wild-type CTF sufficient to block cell growth. No aggregation of the mutant CTFs was seen in fully induced cells (data not shown). The normal concentrations and solubilities of the mutant proteins suggests that they are not grossly denatured, since misfolded proteins usually aggregate or are rapidly degraded when overexpressed in wild-type *E. coli*.

The mutants with the strongest binding defects migrated as single bands on native gels, consistent with expectation, but differed in their relative mobilities. The differences in mobility between these mutants probably reflects their oligomeric state or other conformational differences, rather than their charge, since several mutants have the same charge. All of the mutants except G400D and G539D could be shifted to fast-migrating forms in the presence of 500 μM peptide NR (data not shown), indicating that the mutants retain some peptide binding activity. Binding to a low affinity peptide, KW (KWVHLFG; ref. 7) was also determined for wild-type CTF and 11 of the CTF mutants by spun-column chromatography. Mutants defective in binding peptide NR were also defective in binding KW, and mutants that bound NR with nearly wild-type affinities had little or no defect in KW binding. Thus, the phenotypes of the CTF mutants are not peptide-specific.

All of the CTF mutations, in addition to relieving CTF cytotoxicity, reduced or eliminated the aggregation of proteins *in vivo* following induction at 42°C (Fig. 1*B*). In general, there is a correlation between the strength of the peptide binding defects of the mutant CTFs *in vitro* and the extent to which aggregation is relieved during CTF overexpression *in vivo*

To ensure that the native gel electrophoresis screening did not exclude other CTF mutants with peptide binding defects, 12 CTF mutants with wild-type native gel mobilities were shown to bind peptide normally by native gel assay and by spun-column chromatography (data not shown). The CTF coding regions from two mutant plasmids were sequenced and found to have wild-type sequences. Mutants with wild-type native gel mobilities may carry vector mutations that reduce CTF expression to nontoxic levels.

***In Vivo* Effects of the CTF Mutations when Introduced into Full-Length DnaK.** The CTF mutations were next introduced into a plasmid-borne copy of full-length *dnaK* under the control of a synthetic *lac* promoter and screened for their ability to complement a Δ*dnaK* mutant for temperature-sensitive growth (Table 1) and phage λ plating (data not shown). The Δ*dnaK* strain failed to grow at 16°C or 42°C when transformed with vector alone, but grew as well as the isogenic *dnaK*$^+$ strain when transformed with the parent *dnaK*$^+$ plasmid and induced with 20 μM IPTG. The levels of DnaK

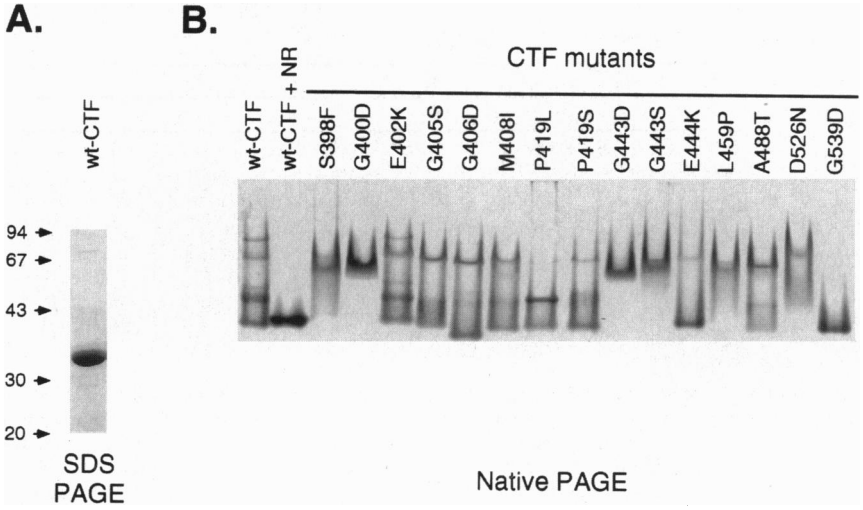

FIG. 2. (*A*) Wild-type CTF purified on Ni^{2+}-NTA agarose and analyzed on an SDS/10% polyacrylamide gel stained with Coomassie blue. The other CTFs were of similar purity. (*B*) Wild-type CTF in the presence or absence of 500 μM NR and mutant CTFs in the absence of peptide were analyzed on 8% native discontinuous polyacrylamide gels stained with Coomassie blue. Protein (4 μg) was loaded in each lane in both *A* and *B*.

Table 1. CTF mutations and their effects on peptide binding by CTF and on cell growth when introduced into full-length *dnaK*

	Mutant alleles of CTF		Mutant alleles of full-length *dnaK*: *In vivo* complementation					
			Δ*dnaK*					
			16°C		42°C		*dnaK*$^+$	
			IPTG, μM		IPTG, μM		IPTG, 50 μM	
Mutation	No. of isolates	Peptide NR binding *in vitro* k_d, μM	20	50	20	50	16°C	42°C
Vector			−	−	−	−	++	++
Wild-type		11	++	+	++	+/−	+/−	+/−
G400D	4	>150	−	−	−	−	+/−	+/−
L459P	2	>150	−	−	−	−	+/−	+/−
G443D	3	>150	−	+	−	−	++	+/−
G443S	2	>150	+/−	+	−	−	+	+
S398F	1	70	+/−	+/−	+/−	+/−	++	+
G539D	3	30	−	+/−	−	+/−	++	+
P419L	6	28	+/−	+/−	−	+/−	+/−	+
P419S	2	20	+/−	−	+	+	+/−	+
E444K	4	28	+/−	++	+	+	+	+
M408I	1	18	−	+/−	++	+	+	+
G405S	1	11	+/−	+	++	+/−	+	+
G406D	1	11	++	+/−	+	−	+/−	+/−
E402K	3	14	+/−	−	++	+	−	+
A488T	3	10	++	−	+	−	−	−
D526N	1	8	+	−	+	−	−	−

Mutations are designated by the single letter code for the wild-type amino acid, its position in the *dnaK* coding sequence, and the single letter code for the substituted amino acid; hence S398F designates the mutation Ser-398 → Phe. In addition to the missense mutations listed, five amber mutations were identified by sequencing: Q433Am, Q442Am, Q456Am, Q471Am, and the double mutant S434F/Q442Am. The affinities of the purified wild-type and mutant CTFs for binding peptide NR were determined by equilibrium dialysis. Measurements for each CTF were made two or three times. Values of calculated K_d's varied by no more than 50% among experiments. Values shown are the average of all determinations. Complementation of the growth defects of a Δ*dnaK* strain by plasmids expressing the corresponding mutant alleles of full-length *dnaK* was screened at 16°C, 30°C, 39°C, and 42°C in the presence of 20, 50, 100, or 200 μM IPTG. Growth at each temperature was scored relative to a *dnaK*$^+$ strain transformed with vector alone and plated on 20 μM IPTG: ++, colonies the size of wild-type; +, colonies smaller than wild-type; +/−, very small (point) colonies; −, no colonies. For clarity, some data are omitted and summarized: (*i*) all Δ*dnaK* and *dnaK*$^+$ transformants grew equally well (++) at 30°C on 20 and 50 μM IPTG; (*ii*) all *dnaK*$^+$ transformants grew equally well (++) at 16°C and 42°C on 20 μM IPTG; (*iii*) data for growth of all transformants at 39°C is similar to the data for 42°C; (*iv*) growth was impaired or blocked for all transformants expressing wild-type or mutant DnaK at 100 or 200 μM IPTG.

expressed from the *dnaK*$^+$ plasmid and the mutant derivatives were equivalent after 1.5 h induction with 20 μM IPTG at 42°C (data not shown). Thus, *dnaK* mutants that fail to complement the Δ*dnaK* strain due so because of functional defects rather than reductions in cellular DnaK concentrations.

Only two *dnaK* mutants, G400D and L459P, failed to complement the Δ*dnaK* strain for growth at both 16°C and 42°C (Table 1) or to support the propagation of λ at 30°C (data not shown). Two other *dnaK* mutant alleles, G443D and G443S, allowed Δ*dnaK* to grow at 16°C but not at 42°C. Note that CTFs carrying these four mutations were the most defective in peptide binding. Failure to complement did not result from toxicity of the mutant DnaK proteins, since an isogenic *dnaK*$^+$ strain carrying the wild-type or the mutant plasmids grew equally well (Table 1). The G539D *dnaK* mutation, which also strongly impaired CTF peptide binding, complemented Δ*dnaK* at 16°C and 42°C at 50 μM IPTG, but not at 20 μM IPTG. Increased levels of G539D DnaK may compensate by mass action for a reduced substrate affinity. The remaining mutations, which, in CTF, had little effect on peptide binding, did not dramatically reduce complementation when placed into full-length *dnaK*. In summary, we find a correlation between the *in vitro* phenotypes of the mutant CTFs and the ability of the corresponding mutant full-length *dnaK's* to complement a Δ*dnaK* strain.

The levels of wild-type or mutant DnaK induced at IPTG concentrations of 50 μM or higher slowed or inhibited growth in both the Δ*dnaK* and *dnaK*$^+$ strain backgrounds. DnaK overexpression has been observed previously to impair cell growth (42, 43). Although several mutant DnaK's were less toxic than the wild-type protein in the *dnaK*$^+$ strain, overexpression of all of the mutant DnaK's inhibited cell growth. Thus, all the mutants retain some of the functional properties of wild-type DnaK *in vivo* (Table 1).

DISCUSSION

The locations of the mutations that impair peptide binding are shown in the cocrystal structure of a slightly truncated form of CTF (residues 389–607) complexed with peptide NR (Fig. 3; ref. 27). Strikingly, six of the mutations cluster in a tightly packed region of the CTF consisting of loop $\mathcal{L}_{1,2}$, loop $\mathcal{L}_{4,5}$, and the β1 strand (Fig. 2). Loop $\mathcal{L}_{1,2}$ is one of the two loops making direct contact with peptide. Loop $\mathcal{L}_{4,5}$ positions and stabilizes loop $\mathcal{L}_{1,2}$, and the β1 strand flanks and makes stabilizing contacts with loop $\mathcal{L}_{4,5}$. Three of the mutations in residues Met-408, Ser-398, and Glu-444 are predicted to eliminate or disrupt stabilizing contacts within the region. The side chain of Met-408, the only residue in the peptide binding loop targeted by a mutation, actually points away from bound peptide toward loop $\mathcal{L}_{4,5}$, where it is the key side chain forming the hydrophobic core between the loops. The hydroxyl group of Ser-398 forms a hydrogen bond with the carboxylate group of Glu-444, connecting the β1-strand to loop $\mathcal{L}_{4,5}$. Mutations at Gly-400 in the β1-strand and Gly-443 in loop $\mathcal{L}_{4,5}$, which confer strong phenotypes, may interfere with the packing of the peptide binding domain. Gly-443 adopts a glycine-specific backbone conformation (ϕ,ψ = 157°, −178°), and replacement of glycine

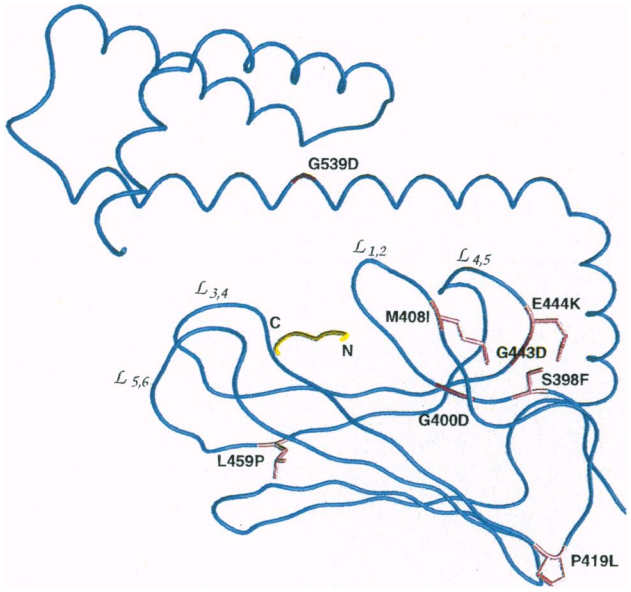

FIG. 3. Distribution of mutations in the three-dimensional structure of CTF. The side chain and carbon backbone atoms of the wild-type residues targeted by mutations are shown, colored either in magenta or, for glycines, in purple. Bound peptide NR is shown in yellow. The model was displayed using GRASP (44).

with either aspartic acid or serine would be energetically unfavorable. Both Gly-400 and Gly-443 lie at the points in the inner two strands of the upper β-sheet closely flanked by the outer two β-strands (β2 and β5). Replacing either with a residue carrying a longer side chain would result in a steric clash with the flanking outer β-strands.

The remaining three sites of mutations that affect peptide binding, Leu-459, Gly-539, and Pro-419, are scattered in the CTF structure, and mutations at each probably result in the distortion of contacts with peptide NR or the peptide binding loops. Leu-459 lies below the peptide binding site in the β5-strand and makes backbone hydrogen bonds and hydrophobic contacts with residues that in turn contact bound peptide. The backbone conformation of Leu-459 is also not favorable for replacement by proline, as in the L459P mutant ($\phi = -120°$). Gly-539 lies in helix αB directly above the peptide binding site, adjacent to the hinge region in helix αB. Finally, Pro-419 is the sole residue in the turn between the β2- and β3-strands that connects the lower and upper β-sheets. Pro-419 adopts a cis-conformation, unfavorable for the substitution of other residues, and is probably required for the sharp turn between the two strands.

Point mutations in residues directly contacting peptide NR were not isolated. Our selection scheme presumably favors mutations affecting the binding of many *in vivo* substrates, and mutations in the binding pocket itself may interfere only with specific substrates or may be compensated for by other binding contacts. Since extensive hydrogen bonding between CTF and the peptide backbone contributes a significant part of the binding energy (27, 45), single missense mutations could have a negligible effect on binding. The mutagenic specificity of hydroxylamine may also have reduced the spectrum of mutations that could be isolated. Mutations affecting substrate binding that lie outside of a binding site have been identified in other proteins, such as the mutation MalE322 in the hinge region of the *E. coli* maltodextrin-binding protein (46).

The clustering of the CTF mutations affecting peptide binding makes an independent, functional argument for the model proposed in our structural analysis of CTF (27). We suggested that the opening and closing of the peptide binding site is achieved by conformational changes in the outer helix and loops of CTF, while the inner helix and loops remain fixed. Though both loops $\mathcal{L}_{1,2}$ and $\mathcal{L}_{3,4}$ make direct contacts with peptide NR, mutations affecting peptide binding were identified only in the region that stabilizes loop $\mathcal{L}_{1,2}$. If the region around loop $\mathcal{L}_{1,2}$ is rigid, it should not easily accommodate distortions induced by mutations. In contrast, mutations in a flexible region able to accommodate distortions by assuming alternative conformations would confer no selectable phenotype. The model can now be further tested by site-directed mutagenesis of the CTF, crystallographic analysis of the mutants, and solution NMR studies of the wild-type protein.

We thank Ulla Beauchamp and the other staff of the Institute of Cancer Research DNA Facility for oligonucleotide synthesis and automated sequencing, Bernd Bukau for providing strain BB1553, John McCarty and Graham Walker for providing plasmid pJM2 and unpublished data, Zhongmin Guo for assistance with CTF mutant screening, and Daved Fremont for assistance with computer graphics. This work was supported by National Institutes of Health Grants GM37219 (M.E.G.) and GM34102 (W.A.H.).

1. Gething, M.-J. & Sambrook, J. (1992) *Nature (London)* **355,** 33–45.
2. Hendrick, J. P. & Hartl, F.-U. (1993) *Annu. Rev. Biochem.* **62,** 349–384.
3. Craig, E. A., Gambill, B. D. & Nelson, R. J. (1993) *Microbiol. Rev.* **57,** 402–414.
4. Morimoto, R. I., Tissières, A. & Georgopoulos, C. (1994) *The Biology of Heat Shock Proteins and Molecular Chaperones* (Cold Spring Harbor Lab. Press, Plainview, NY), pp. 1–30.
5. Flynn, G. C., Pohl, J., Flocco, M. T. & Rothman, J. E. (1991) *Nature (London)* **353,** 726–730.
6. Blond-Elguindi, S., Cwirla, S. E., Dower, W. J., Lipshutz, R. J., Sprang, S. R., Sambrook, J. F. & Gething, M.-J. H. (1993) *Cell* **75,** 717–728.
7. Gragerov, A., Zeng, L., Zhao, X., Burkholder, W. & Gottesman, M. E. (1994) *J. Mol. Biol.* **235,** 848–854.
8. McCarty, J. S., Rüdiger, S., Schönfeld, H.-J., Schneider-Mergener, J., Nakahigashi, K., Yura, T. & Bukau, B. (1996) *J. Mol. Biol.* **256,** 829–837.
9. Palleros, D. R., Welch, W. J. & Fink, A. L. (1991) *Proc. Natl. Acad. Sci. USA* **88,** 5719–5723.
10. Schmid, D., Baici, A., Gehring, H. & Christen, P. (1994) *Science* **263,** 971–973.
11. Palleros, D. R., Shi, L., Reid, K. L. & Fink, A. L. (1994) *J. Biol. Chem.* **269,** 13107–13114.
12. Szabo, A., Langer, T., Schröder, H., Flanagan, J., Bukau, B. & Hartl, F. U. (1994) *Proc. Natl. Acad. Sci. USA* **91,** 10345–10349.
13. Greene, L. E., Zinner, R., Naficy, S. & Eisenberg, E. (1995) *J. Biol. Chem.* **270,** 2967–2973.
14. McCarty, J. S., Buchberger, A., Reinstein, J. & Bukau, B. (1995) *J. Mol. Biol.* **249,** 126–137.
15. Palleros, D. R., Reid, K. L., Shi, L., Welch, W. J. & Fink, A. L. (1993) *Nature (London)* **365,** 664–666.
16. Liberek, K., Skowyra, D., Zylicz, M., Johnson, C. & Georgopoulos, C. (1991) *J. Biol. Chem.* **266,** 14491–14496.
17. Banecki, B., Zylicz, M., Bertoli, E. & Tanfani, F. (1992) *J. Biol. Chem.* **267,** 25051–25058.
18. Palleros, D. R., Reid, K. L., McCarty, J. S., Walker, G. C. & Fink, A. L. (1992) *J. Biol. Chem.* **267,** 5279–5285.
19. Buchberger, A., Theyssen, H., Schröder, H., McCarty, J. S., Virgallita, G., Milkereit, P., Reinstein, J. & Bukau, B. (1995) *J. Biol. Chem.* **270,** 16903–16910.
20. Wilbanks, S. M., Chen, L., Tsuruta, H., Hodgson, K. O. & McKay, D. B. (1995) *Biochemistry* **34,** 12095–12106.
21. Chappell, T. G., Konforti, B. B., Schmid, S. L. & Rothman, J. E. (1987) *J. Biol. Chem.* **262,** 746–751.
22. Wang, T.-F., Chang, J.-h. & Wang, C. (1993) *J. Biol. Chem.* **268,** 26049–26051.
23. Wawrzynów, A. & Zylicz, M. (1995) *J. Biol. Chem.* **270,** 19300–19306.
24. Tsai, M.-Y. & Wang, C. (1994) *J. Biol. Chem.* **269,** 5958–5962.
25. Freeman, B. C., Myers, M. P., Schumacher, R. & Morimoto, R. I. (1995) *EMBO J.* **14,** 2281–2292.
26. Zhang, J. & Walker, G. C. (1996) *J. Biol. Chem.* **271,** in press.

27. Zhu, X., Zhao, X., Burkholder, W. F., Gragerov, A., Ogata, C. M., Gottesman, M. E. & Hendrickson, W. A. (1996) *Science* **272,** 1606–1614.
28. Bukau, B. & Walker, G. (1990) *EMBO J.* **9,** 4027–4036.
29. Miller, J. H. (1972) *Experiments in Molecular Genetics* (Cold Spring Harbor Lab. Press, Plainview, NY).
30. McCarty, J. S. & Walker, G. C. (1991) *Proc. Natl. Acad. Sci. USA* **88,** 9513–9517.
31. Humphreys, G. O., Willshaw, G. A., Smith, H. R. & Anderson, E. S. (1976) *Mol. Gen. Genet.* **145,** 101–108.
32. Paek, K. H. & Walker, G. C. (1987) *J. Bacteriol.* **169,** 283–290.
33. Gragerov, A., Nudler, E., Komissarova, N., Gaitanaris, G. A., Gottesman, M. E. & Nikiforov, V. (1992) *Proc. Natl. Acad. Sci. USA* **89,** 10341–10344.
34. Ueguchi, C., Shiozawa, T., Kakeda, M., Yamada, H. & Mizuno, T. (1995) *J. Bacteriol.* **177,** 3894–3896.
35. Kim, H., Lee, Y. J. & Corry, P. M. (1992) *J. Cell. Physiol.* **153,** 353–361.
36. Freiden, P. J., Gaut, J. R. & Hendershot, L. M. (1992) *EMBO J.* **11,** 63–70.
37. Blond-Elguindi, S., Fourie, A. M., Sambrook, J. P. & Gething, M.-J. H. (1993) *J. Biol. Chem.* **268,** 12730–12735.
38. Román, E., Moreno, C. & Young, D. (1994) *Eur. J. Biochem.* **222,** 65–73.
39. Takenaka, I. M., Leung, S.-M., McAndrew, S. J., Brown, J. P. & Hightower, L. E. (1995) *J. Biol. Chem.* **270,** 19839–19844.
40. Shi, L., Kataoka, M. & Fink, A. L. (1995) *Biochemistry* **35,** 3297–3308.
41. Benaroudj, N., Batelier, G., Triniolles, F. & Ladjimi, M. M. (1995) *Biochemistry* **34,** 15282–15290.
42. Blum, P., Ory, J., Bauernfeind, J. & Krska, J. (1992) *J. Bacteriol.* **174,** 7436–7444.
43. Buchberger, A., Valencia, A., McMacken, R., Sander, C. & Bukau, B. (1994) *EMBO J.* **13,** 1687–1695.
44. Nicholls, A., Sharp, K. A. & Honig, B. (1991) *Proteins Struct. Funct. Genet.* **11,** 281–296.
45. Landry, S. J., Jordan, R., McMacken, R. & Gierasch, L. M. (1992) *Nature (London)* **355,** 455–457.
46. Sharff, A. J., Rodseth, L. E., Szmelcman, S., Hofnung, M. & Quiocho, F. A. (1995) *J. Mol. Biol.* **246,** 8–13.